# INTERPRETATION OF SPECTROMETRIC MEASUREMENTS OF ACTIVE GEOSTATIONARY SATELLITES

Donald Bédard*, Gregg A. Wade†
*Royal Military College of Canada, Kingston, Canada*
Andrew Jolley‡
*Defence Space Coordinating Office, Canberra, Australia*

**Abstract**

Over 5000 visible near-infrared (VNIR) spectrometric measurements of active geostationary satellites have been collected with the National Research Council (NRC) 1.8m Plaskett telescope located at the Dominion Astrophysical Observatory (DAO) in Victoria, Canada. A little more than 2000 addtional measurements were collected with the 1.6m telescope of the *Observatoire du Mont Mégantic* (OMM) located about 200 km to the south-east of Montréal, Canada. The objective of this ongoing experiment is to study how reflectance spectroscopy can be used to reliably identify specific material types on the surfaces of artificial Earth-orbiting objects. Active geostationary satellites have been selected as the main subjects for this experiment since their orientation is stable and can be estimated with a high-level of confidence throughout a night of observation. Furthermore, for most geostationary satellites, there is a wide variety of sources that can provide some level of a priori information as to their external surface composition. Notwithstanding the high number of measurements that have been collected to date, it was assumed that the experimenters would have a much greater success rate in material identification given the choice experimental subjects. To date, only the presence of aluminum has been confidently identified in some of the reflectance spectra that have been collected. Two additional material types, namely photovoltaic cells and polyimide film, the first layer of multi-layer insulation (MLI), have also been possibly identified. However uncertainties in the reduced spectral measurements prevent any definitive conclusion with respect to these materials at this time. The surprising lack of unambiguous detection of surface materials leads us to propose other data interpretation methods to characterize the spectral scattering characteristics of the studied satellites.

## 1 INTRODUCTION

Today, there are over 17,000 artificial objects in Earth orbit of which only approximately 2,000 are operational spacecraft. The remainder of these objects are space debris. Some of these space debris objects are well known and include spent rocket bodies, dead satellites or mission-related debris such as optical telescope covers. However, there are many space debris objects for which we have no information as to what they are or from which mission they originated with. An example of such space debris objects are the high-area-to-mass-ratio (HAMR) objects that were first discovered by Schildknecht et al. [1, 2]. While it is believed that these pieces may be multi-layer insulation (MLI), to date no one has provided conclusive evidence that this is the case. From a scientific and civil perspective, the ability to identify specific material types on the surface of space debris objects may allow researchers to positively identify the material makeup of such objects, such as the HAMR, and then retrace their origin to a specific source. Not only would this information be useful to improve orbit prediction models for these debris objects but might also prove extremely valuable in limiting future sources of debris by improving spacecraft and launch vehicle designs.

From a defence and security perspective, the identification of specific types of materials on active spacecraft could represent an additional piece of information to increase the level of space situational awareness (SSA) senior decision makers have at their disposal. For example, this type of information could be used to confirm

*Major, Space Surveillance Research Laboratory, Department of Physics, donald.bedard@rmc.ca
†Professor, Space Surveillance Research Laboratory, Department of Physics, gregg.wade@rmc.ca
‡Squadron Leader, Royal Australian Air Force, andrew.jolley@defence.gov.au

the identity of a specific satellite or in the case of unknown satellites, confirm the material composition of some of its reflecting components which could then be used to understand which organization owns the spacecraft.

Reflectance spectroscopy is an important tool that has been used by planetary scientists to learn about the compositional nature of planetesimals in our solar systems. By comparing spectra of asteroids to those of other asteroids and common minerals found on Earth, these scientists have been able to determine the composition of these small bodies and thus learn more about the origin and nature of these celestial objects [3]. Although astronomical geologists have successfully used astronomical reflectance spectroscopy to investigate the mineralogical composition of asteroids for more than three decades, the use of this observational technique to characterize surface material composition of artificial space objects, namely active spacecraft and space debris objects, is still in its infancy. Previous efforts in the field of spectrometric characterization of artificial Earth-orbiting objects [4–11] have endeavoured to identify specific material types from spectral reflectance measurements at visible wavelengths by comparing the continuum slope of a limited set of measurements to those of materials characterized in a laboratory environment. With the exception of a few observations, most analyses of spectra discussed in the literature concern space debris, objects for which there is no information on their attitude state and whose surface characteristics may have suffered non-negligible alterations since their launch. All of these experiments have shown that the determination of material types from reflectance spectra obtained from space debris objects is not a trivial task and that many more experiments are required to determine if this is a viable technique.

This paper presents an observational experiment that was focused on collecting spectra of active geostationary satellites to specifically detect the presence of solar cells and MLI, two very common material types found on the surfaces of spacecraft. The measurements used for this experiment were collected with the 1.8m Plaskett telescope located at the Dominion Astrophysical Observatory (DAO) in Victoria, Canada and the 1.6m telescope of the *Observatoire du Mont Mégantic* (OMM) located about 200 km to the south-east of Montréal, Canada. The paper begins with a brief review of previous research work applicable to the experiment presented herein and explains the reasoning for the selection of the experimental aim. The next two sections discuss the experiment objectives, the experimental setup and the objects that were observed. The paper then continues with an explanation of the data reduction procedure. Results are then presented and the paper concludes with a description of the future work that will follow the experiment presented here.

## 2 PREVIOUS WORK

Previous scientific work related to the research presented here has been categorized into two groups: laboratory characterization of spacecraft and laboratory characterization of homogenous spacecraft materials.

### 2.1 LABORATORY CHARACTERIZATION OF SPACECRAFT

The characterization of the CanX-1 engineering model (EM) experiment conducted by Bédard and Lévesque [12] successfully demonstrated that the reflected light from the surface of a small cubesat with a simple exterior design could be measured in a laboratory to determine the composition of the surface materials from measured spectra with no *a priori* data on the object under study. For this experiment, the CanX-1 EM consisted of a 10 cm cubesat mainly covered by triple-junction photovoltaic (TJPV) cells and one bare aluminum panel. Although this experiment doesn't answer whether reflectance spectroscopy can be used to identify material types on more complex spacecraft in space, the experiment's outcome was nonetheless a positive step in that direction.

Another key observation from this experiment that was deemed useful for the planning of an observational experiment was that specularly reflecting materials covering the CanX-1 EM could only be detected when the spectrometric detector was located within the specular reflection region. Outside of specular geometries, the solar cells and the bare aluminum panel were not detected since, simply put, sufficient light was not reflected toward the detector. Applying this to an experiment to observe satellites in situ, spectra for solar cells and other specular materials such as MLI will only be detected in favourable observational geometries.

### 2.2 LABORATORY CHARACTERIZATION OF SPACECRAFT MATERIALS

The second research effort that was used to prepare for the observational experiment was the measurement of the spectral bidirectional reflectance distribution function (BRDF) of spacecraft materials commonly found on the surfaces of satellites. The details of this research activity including the instrument and experiment

setup, the data collection and processing procedure as well as complete description of the results are described by Bédard [13]. As part of this work, material samples consisting of four types of materials were characterized, namely TJPV cells, aluminized polyimide films, bare aluminum panels and white-coated aluminum panels. The remainder of this section summarizes the key findings from this research activity that were applicable to the observational experiments conducted at the DAO and OMM.

The spectral BRDF of TJPV cells are very distinctive compared to other materials for which spectra were obtained. As shown in Fig. 1, all four TJPV cells showed very different spectral BRDFs albeit with one similar trait: all measurements exhibited interference fringes above a wavelength of 800 nm. As noted by Bédard and Lévesque [12], this interference pattern is caused by the multiple layer of semi-conductors that comprise each individual cell. It was also noted during that experiment that all studied TJPV cells proved to be very specular, even in the case of a cell with a poor surface condition. From a practical point of view when planning an observational experiment of active geostationary satellites, detection of solar cell spectra should only be feasible when these surfaces are in a geometry suitable to specularly reflect sunlight in the direction of the observer.

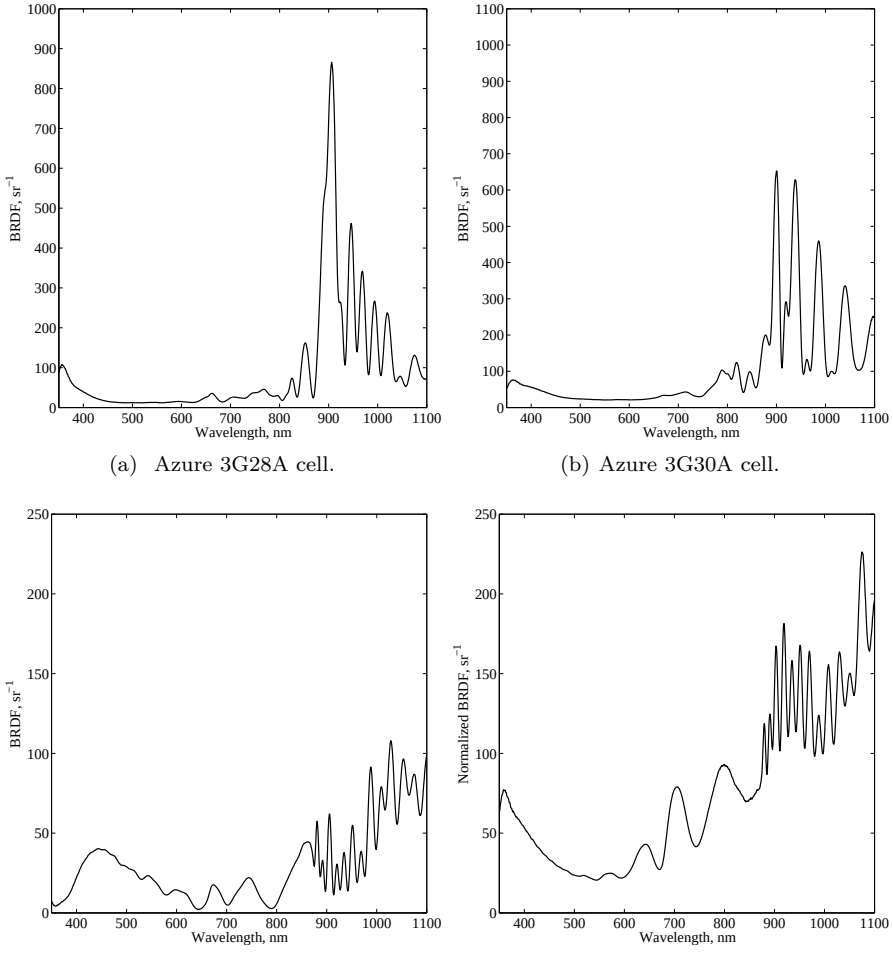


(a) Azure 3G28A cell.

(b) Azure 3G30A cell.

(c) CanX-1 EM Emcore cell.

(d) Quicksat Emcore cell.

**Figure 1: BRDF measurements of four different TJPV cells all taken at an incidence angle, $\theta_i = 30^\circ$ and a reflection angle, $\theta_r = 30^\circ$.**

Aluminized polyimide films, which are commonly used as the first layer in MLI, also have a very distinct spectral BRDF which might prove easily identifiable in reflectance spectra of artificial Earth-orbiting object. Figure 2 shows the spectral BRDF of two different aluminized polyimide film samples. The one illustrated in Fig. 2(a) is a pristine sample which showed no surface degradation while the measurements illustrated in Fig.

2(b) were obtained from a degraded and very wrinkled sample. In either case, the spectral energy distribution (SED) of the BRDF was very familiar, both showing the marked increase in reflectivity at wavelengths greater than 500 nm. Moreover, both samples showed a fringing pattern caused by multilayer reflection. This feature is not surprising since this type of material is composed of a thin layer of aluminum on a thin sheet of polyimide film. In addition to these characteristics, the aluminum absorption feature centered at approximately 850 nm is easily observed in both film samples. Finally, like the TJPV cell samples, the aluminized polyimide films proved to be very specular reflecting surfaces. Applying this result to an observational experiment signifies that this type of material would only be visible when reflecting directly in the direction of the sensor.

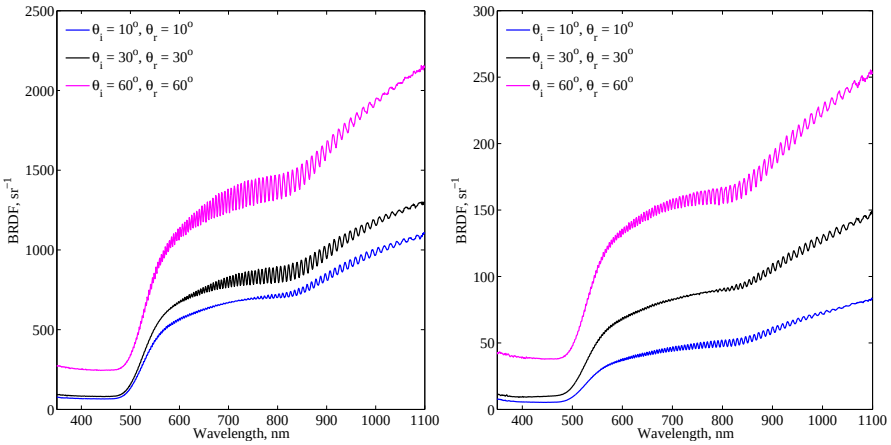


(a) Pristine film. (b) Degraded film.

**Figure 2: Spectral BRDF of two different aluminum coated polyimide films.**

The last two measurements presented in Fig. 3 are from two aluminum samples. The first one consisted of a bare first-surface aluminum mirror while the second was coated with a low-outgassing white paint commonly used on spacecraft. The spectral BRDF for the bare aluminum mirror in Fig. 3(a) shows a practically featureless spectrum other than the common aluminum absorption feature centered on 850 nm. It is noted here that the detection of an aluminum absorption feature at this wavelength in the reflectance spectra of a spacecraft would confirm the presence of aluminum which could either be associated with a bare aluminum surface or an aluminized polyimide film. The spectral BRDF of the white-coated aluminum panel in Fig. 3(b) shows a completely featureless spectrum between 450 and 1100 nm which would make it practically impossible to identify based on this type of data alone within this specific spectral range.

## 3 EXPERIMENT AIM

The aim of the experiment was to detect the presence of TJPV cells and MLI in reflectance spectra of active spacecraft. This specific aim was selected for two reasons. First, most spacecraft that are in Earth-orbit today have solar cells and MLI covering a significant portion of their surface. Second, the laboratory experiments presented in Section 2 have shown that these material types should be easily detectable due in part to their specular nature and their distinct spectral BRDF.

Two requirements were deemed essential in order to maximize the likelihood of detecting the presence of solar cells and MLI in spacecraft reflectance spectra. First, observations would be limited to artificial space objects whose Sun-object-sensor geometry changed negligibly over a 60 to 90 second exposure time. This requirement effectively limited the range of subjects to active geostationary satellites that are 3-axis stabilized. More specifically, communications and weather satellites in geostationary orbits typically have three-axis stabilized buses with their antennas pointed towards fixed points on Earth while their solar panels are tracking the Sun.

Second, since there is no method of knowing when the materials of interest would reflect specularly toward the detector used for the experiment, the second experimental requirement was to collect multiple spectra of each studied satellite over an entire night. Therefore, time-resolved spectrometric measurement was also

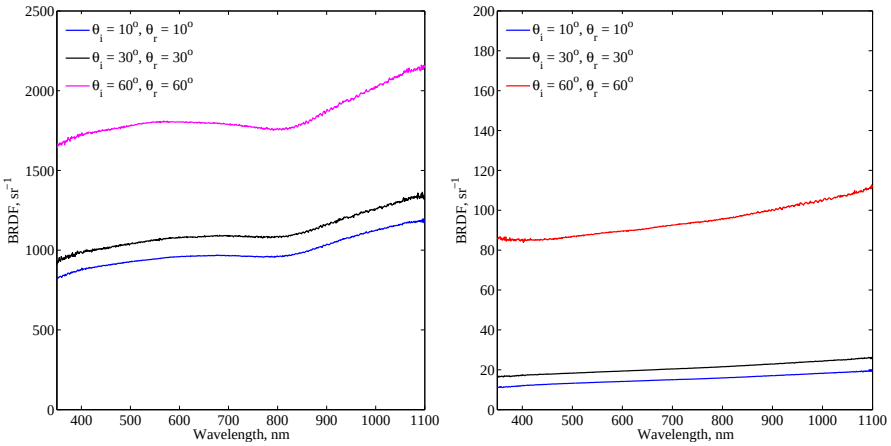


(a) Bare aluminum mirror. (b) White-coated aluminum panel.

**Figure 3: Spectral BRDF of a bare aluminum mirror and a white-coated aluminum panel.**

believed to be a factor that would increase the probability of detecting the materials of interest for a given satellite.

## 4 EXPERIMENT SETUP AND PROCEDURE

Results presented in this paper were derived from measurements obtained at two sites, namely at the Dominion Astrophysical Observatory (DAO) in Victoria, British Columbia and the *Observatoire du Mont Mégantic* (OMM) located approximately 200 km South-East of Montréal in Québec.

The 1.8-metre telescope at the DAO is equipped with a Cassegrain spectrograph [14]. The instrument configuration that was selected for this experiment provided a wavelength range of approximately 330 nm for a given grating angle at a low spectral resolving power (R $\approx$ 200). The 1.8-metre telescope is not equipped with an atmospheric dispersion corrector (ADC) and as such a very wide 30 x 18 arcsecond slit was used to ensure that most of the visible light would reach the spectrograph. The measurements were captured with a UV-coated SITe-2 CCD (1752 x 532 pixels, 15 micron square pixels) with a nominal operating temperature of -110$^o$ C.

The spectrograph on the OMM 1.6-meter Ritchey-Chrétien telescope provides the opportunity to configure it such that it provides a spectral range of approximately 430 nm which is significantly greater than that obtained at the DAO. Like the latter, the grating angle can be varied to collect measurements anywhere between 350 and 950 nm. The detector is an STA0520A CCD (2688 x 512 pixels, 15 micron square pixels) with a nominal operating temperature of -115$^o$ C. Contrary to the DAO 1.8m telescope, the OMM one is equipped with an ADC and thus a smaller slit size, namely 8 arcseconds, was used for the observational experiment.

The first type of data collected were the spectrometric measurements of the active geostationary satellites. The typical exposure time at both observatories ranged between 30 and 60 seconds. This range of exposure time was selected as a compromise between the requirement to keep the exposure time as short as possible such that the observational geometry did not vary significantly during the exposure and the requirement to obtain a sufficient signal-to-noise ratio (SNR) at times at which the satellite appeared faintest. Table 1 provides a list of the geostationary satellites for which results are presented in this paper.

Three other types of CCD frames were collected during each night of observations. The first consisted of sequences of bias and flat field frames required for the data reduction process. Second, measurements of spectrophotometric standards stars [15] well as solar analogue stars [16], located at air masses similar to the spacecraft of interest, were gathered in order to retrieve the intrinsic reflectance of the observed spacecraft. In order to obtain measurements of these astronomical standards, spacecraft observations were typically interrupted during the night for 10 to 20 minutes. While the instrument configuration for the observations of the spectrophotometric standards and solar analogues remained unchanged, the exposure time for each specific star was adjusted such that each frame would be in the region of linearity of the CCD.

Table 1: Geostationary satellites for which results are presented in this paper.

| Spacecraft | Satellite Catalog # | Air mass | Bus | Launched | Observation site | Date of observation |
|---|---|---|---|---|---|---|
| GOES 15 | 36411 | 1.799 | BSS-601 | Mar 2010 | DAO | 22 Aug 2012 |
| Anik F1 | 26624 | 1.875 | BSS-702 (with solar concentrators) | Nov 2000 | DAO | 21 Aug 2014 |
| Ciel 2 | 33453 | 1.782 | Spacebus 4000C4 | Dec 2008 | DAO | 17 Aug 2014 |
| Anik G1 | 39127 | 1.876 | LS-1300 (expanded) | Apr 2013 | DAO | 11 Mar 2014 |
| XM 1 | 26761 | 1.721 | BSS-702 (with solar concentrators) | May 2001 | OMM | 22 Jul 2014 |

## 5 DATA REDUCTION PROCEDURE

At the start of the data reduction procedure, all observations were subjected to the preliminary data reduction stage in order to convert the raw data data into one-dimensional spectra containing information only from the sunlight reflected from the satellite of interest. The first part of this process consists in removing the instrumental signature from the data. As such, all measurements were processed for bias removal, flat-field correction as well as cosmic ray hit removal using the *ccdproc* task in the IRAF package developed by the NOAO. This procedure has been described in great details by Massey [17]. The second part consists in extracting a one-dimensional spectrum from the two-dimensional data array collected by the CCD detector. The tasks involved include the extraction of the spectrum, performing a wavelength calibration and finally performing a flux calibration. The second part of the procedure has also been thoroughly explained by Massey et al. [18].

Once the raw data was processed, all remaining data processing was performed using MATLAB which is a commercial software package. The remaining data processing steps included producing broadband photometric light curves from the time-resolved spectra, scaled reflectance spectra, relative reflectance spectra and finally time-resolved colour ratios from the time-resolved spectra.

### 5.1 PHOTOMETRIC LIGHT CURVE

The production of time-resolved photometric light curves derived from the spectrometric measurements was deemed essential in order to have a proper context within which the individual spectra could be studied. For example, the detection of spectral features associated with solar cells at the brightest point on a light curve could lead to the conclusion that a potential specular reflection from a solar panel had been observed. We calculate the (uncalibrated) photometric brightness of each satellite as a function of time by computing the total flux from each spectrum, $F_{total}(t)$, taken at time $t$ and integrated over the wavelength region between $\lambda_1$ and $\lambda_2$ as follows:

$$F_{\text{total}}(t) = log_{10} \sum_{\lambda_1}^{\lambda_2} S_{\text{sat}}(\lambda; t) \tag{1}$$

where $S_{\text{sat}}(\lambda; t)$ is the measured signal in ADU. Each flux measurement was plotted as a function of the time to produce a time-resolved broadband photometric light curve of the object.

### 5.2 SCALED REFLECTANCE SPECTRA

The next data product that was derived from the spectra was normalized reflectance spectra which are the main data used to identify the presence of specific material types. This data product is comparable to that used by all of the teams that have collected spectrometric measurements of artificial space objects as previously described [5–11]. The procedure used to obtain normalized reflectance spectra is also the same method used to reduce asteroid spectra and is described in detail by Bus *et al.* [19].

The reflectance of a spacecraft $R_{sat}(\lambda)$, is obtained by dividing the measured signal in ADU of the satellite, $S_{\text{sat}}(\lambda)$, by that of a solar analogue, $S_{\text{SA}}(\lambda)$, as follows:

$$R_{\text{sat}}(\lambda) = \frac{S_{\text{sat}}(\lambda)}{S_{\text{SA}}(\lambda)} \tag{2}$$

In order to facilitate the comparison of multiple reflectance spectra of the same satellite, all the reflectance spectra were then normalized to unity at 550 nm.

### 5.3 RELATIVE REFLECTANCE

One of the objectives of the experiment was to evaluate how the SED of a satellite varied over the course of the observation period. The first method that was implemented to satisfy this was to compare various spectra of a specific spacecraft relative to one spectrum, of the same spacecraft, selected as a reference. Since, the satellite remained in the same position in the sky and all measurements were taken at the same airmass, the unnormalized spectral measurements (in ADU) were used for this operation. Mathematically, the relative reflectance, $R_{\text{sat,relative}}(\lambda)$, is expressed as follows:

$$R_{\text{sat,relative}}(\lambda) = \frac{S_{\text{sat}}(\lambda)}{S_{\text{sat,ref}}(\lambda)} \tag{3}$$

As with the spectral reflectance, the relative reflectance measurements were also normalized to unity at 550 nm to facilitate the interpretation of the results. Once this was completed, the normalized relative reflectance measurements allowed for a better visualization as to which part of the spectrum varied compared to a measurement selected as a reference measurement.

### 5.4 COLOUR RATIOS

To properly study the variation of the SED over the course of a complete night of observation, broadband colour ratios were used. This technique, also employed by Bédard and Lévesque [12] during the laboratory characterization of the CanX-1 EM and Bédard [13] for the characterization of homegeneous spacecraft materials, was implemented as the last data reduction step for this observational experiment. To produce the colour ratio, each reduced spectrometric measurement was multiplied by filter transmittance functions (ie., $T_{Blue}$, $T_{Vis}$ and $T_{Red}$) corresponding to the Bessel blue, visual and red (BVR) filters [20]. The reflectance measurements calculated with Equation 2 were used as the inputs so that any atmospheric effects would be removed from the results thereby allowing experimenters to compare ratios from different spacecraft. The filtered reflectances were then integrated over wavelength to compute the total flux in each band from which colour ratios were produced. In mathematical terms, this process is summarized by the following equation:

$$\text{Ratio}(t)_{\text{Colour1/Colour2}} = \frac{\sum S_{\text{sat}}(\lambda;t) \cdot T_{\text{Colour1}}(\lambda)}{\sum S_{\text{sat}}(\lambda;t) \cdot T_{\text{Colour2}}(\lambda)} \tag{4}$$

In total, three colour ratios as a function of time were produced, blue to red (B/R), blue to visible (B/V), and visible to red (V/R). These colour ratios were plotted as a function of time to provide an additional visualization of how the SED varied over the course of each night.

## 6 RESULTS

The following section presents selected results from measurements obtained at the DAO and OMM obervatories between August 2012 and August 2014. The first results that are illustrated in Fig. 4 are derived from measurements of the GOES-15 spacecraft collected on 17 August 2012. The lightcurve for this object allows one to conclude that the measurements did capture the variation in brightness of the satellite over the night. Seven reflectance spectra are given in Fig. 6(a). The identification numbers of the spectra correspond to the numbers that are provided on top of the light curve. It is noted that all of the sampled scaled spectra shown in Fig. 4(b) reveal no distinct spectral features that can be attributed to solar cells or MLI. The colour ratios indicate that there is very little colour variation in the sunlight reflected from the GOES-15 spacecraft over the course of the night. The relative reflectance measurements in Fig. 4(c) show that the spectra collected at times #2 through #6 reflect less at longer wavelengths allowing one to conclude that the Reference measurement and #1 are indivative of a slightly redder material.

The next results shown in Fig. 5 are those of the Anik F1 spacecraft collected with the DAO sensor on 21 August 2014. The broadband photometric lightcurve of this spacecraft has many more features than that of the GOES-15 spacecraft. While the colour ratios show some variability, the scatter of the photometric data prevent any definitive conclusion at this time as to whether these changes are caused by the spacecraft or by atmospheric phenomena. It is still interesting to note the differing variations of colour ratios for the Reference measurements as well as #2 and #3 in Fig. 5(a) that appear to correspond to the increases in brightness seen in the broadband photometric lightcurve. The selected scaled reflectance spectra in Fig. 5(b)

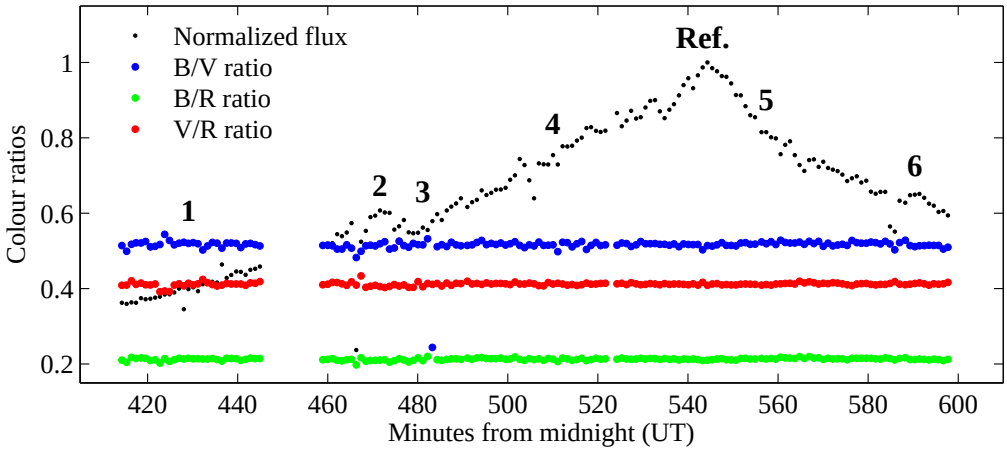


(a) Broadband lightcurve and colour ratios.

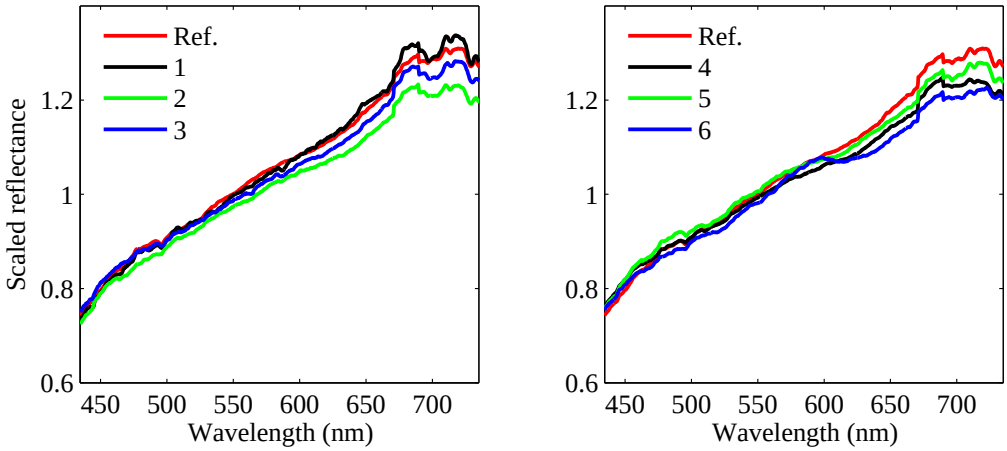


(b) Scaled reflectance spectra.

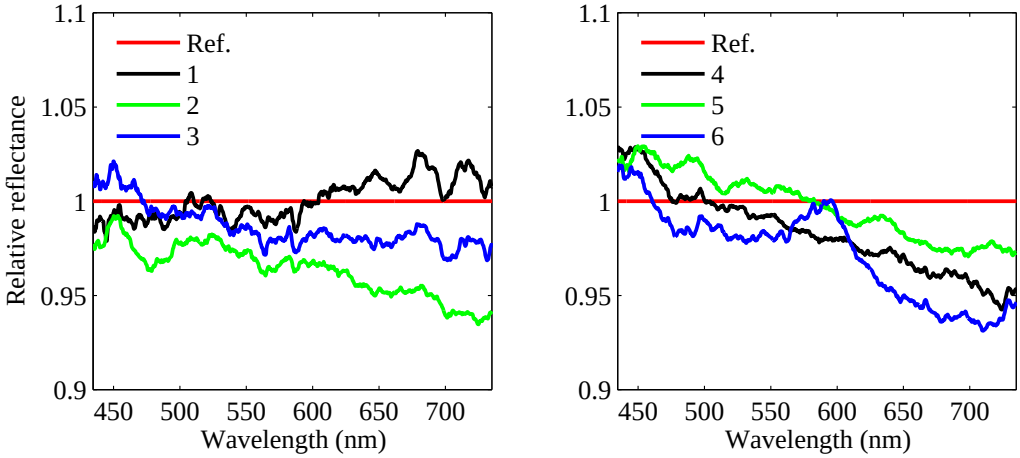


(c) Relative reflectance spectra.

**Figure 4: Measurements of the GOES-15 spacecraft collected with the DAO 1.8m telescope on 22 Aug 2012.**

are featureless and do not offer any easily identifiable spectral characteristics that might resemble those of solar cells or metalized polyimide films. It is noted here that the nature of the broad absorption feature above 700 nm is not recognized and was most likely an atmospheric absorption feature that was improperly removed due to errors in the data reduction process, namely the wavelength calibration and flux calibration. Unfortunately, spectra for only one solar analogue was collected on this evening which prevents the authors from confirming the origin of this feature. Finally, the relative reflectance spectra of the seven measurements do show that there was significant variations in the SED over the course of the night. Interestingly, it is noted that measurements #1 and #2 appear to have a lesser blue content than all others which may be indicative that there is a lesser contribution from solar cell materials at these times.

The third set of results that are presented in Fig. 6 are those of the Ciel-2 satellite taken with the DAO telescope on 21 August 2014. Figure 6(a) provides the broadband photometric lightcurve that was derived from the spectrometric measurements and shows a complex variation with interesting features. As the spacecraft becomes progressively brighter up to the Reference measurements, there are smaller localized increases in brightness centered at measurements #1 to #3 which are indicative of smaller specular reflections. Overall, the clean lightcurve gives confidence that the variation in the various colour ratios are caused by the satellites and not atmospheric factors. However the time-resolved colour ratios do not show significant SED variations over time that could lead to clear conclusions regarding material types. On the other hand, the scaled reflectance spectra of the Ciel-2 spacecraft in Fig. 6(b) is encouraging and show clear bulges below 500 nm, which would give the observed object at these specific observation times a bluish surface. At this point, it is noted that the CanX-1 EM Emcore TJPV, whose spectral BRDF was presented in Fig. 1(c), has a similar spectral feature. While it is unlikely that the Ciel-2 spacecraft has the same type of TJPV as the CanX-1 EM, it is not unreasonable to conclude that the presence of solar cells has most likely been identified in these reflectance spectra. Finally, the relative spectra shown in Fig. 6(c) show that there is a significant vatiation in the SED between measurements. Again, while relative spectra do not provide specific information about material types at each measurement, they do give some clues about the difference in colour between the various measurements and the Reference. For example, measurement #6 appears to have a higher blue content then at any other measurements which leads us to believe that this portion of the lightcurve has a significant component of specular reflections coming off from solar panels.

The following results that are illustrated in Fig. 7 are those of the Anik G1 spacecraft which were obtained with the DAO telescope on 11 March 2014. Contrary to the all of the other DAO results that have been presented previously, the grating angle was changed so as to collect spectra between approximately 600 and 900 nm. The lightcurve presented in Fig. 7 corresponds well to lightcurves of this satellite bus class that were previously published by Vrba et al. [21]. Since the wavelength region of the measured spectra was well above the blue and visual bands, no colour ratios were produced. The scaled reflectance spectra given in Fig. 7(b) clearly show a broad absorption feature above 800 nm, one that can be confidently attributed to the presence of aluminum based on a comparison of this result with those of Figs. 2 and 3. Since it is unlikely that a bare aluminum panel would be present on the surface of the Anik G1 spacecraft, it is believed that this feature is indicative of alumunized polyimide film which is the first layer typically used in MLI blankets. Assuming therefore that our analysis is correct then, surprisingly, this material is detected in all of the seven measurements taken, from the brightest, the Reference measurement, to the dimmest, #6. More surprisingly, at the brightest time when it was expected that the presence of solar cells would be easily be detected, only the spectral feature associated with MLI is observed. A look at Figs. 1 and 2(a) shows that the pristine MLI sample is significantly more reflective, especially above 500 nm, than all of the TJPV cells samples that were characterized and could explain why only the presence of MLI, and not the solar cells, is seen in all of the measurements in Fig. 7(b). This explanation corresponds well with the fact that the MLI on the surface of the Anik G1 spacecraft has most likely not experienced much space weathering since it was launched a little over a year ago.

The final results, given in Fig. 8, are those of the Galaxy 11 spacecraft which were derived from the measurements collected with the OMM telescope on 23 July 2014. The broadband photometric lightcurve shows two brightness peak with a very similar width. Without any information, it could be easily be concluded that the components responsible for these peaks are composed of similar materials, or at least, have similar reflective characteristics. The colour ratios, which provide the most significant variations observed yet, show that the SEDs for these two peaks are similar except for a small difference in the B/V colour ratios, centered at peak intensity. From this data alone, it is unknown if this difference was caused by atmospheric effects

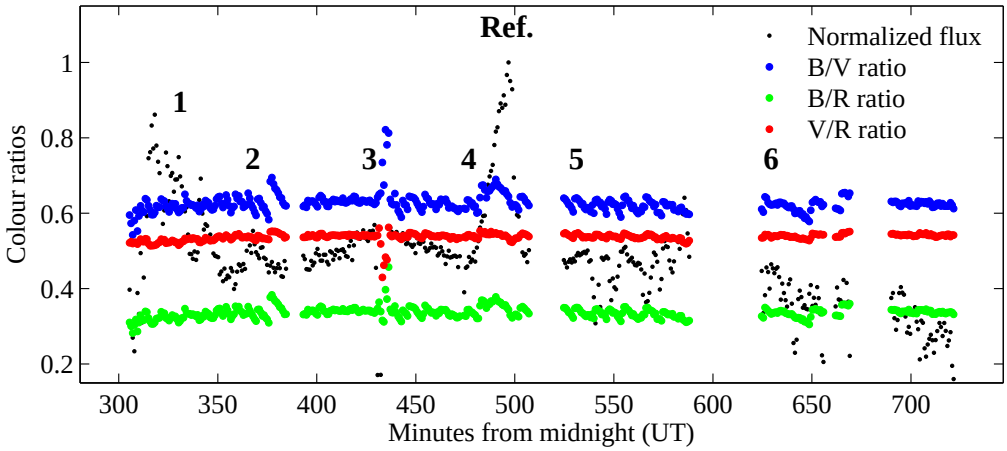


(a) Broadband lightcurve and colour ratios.

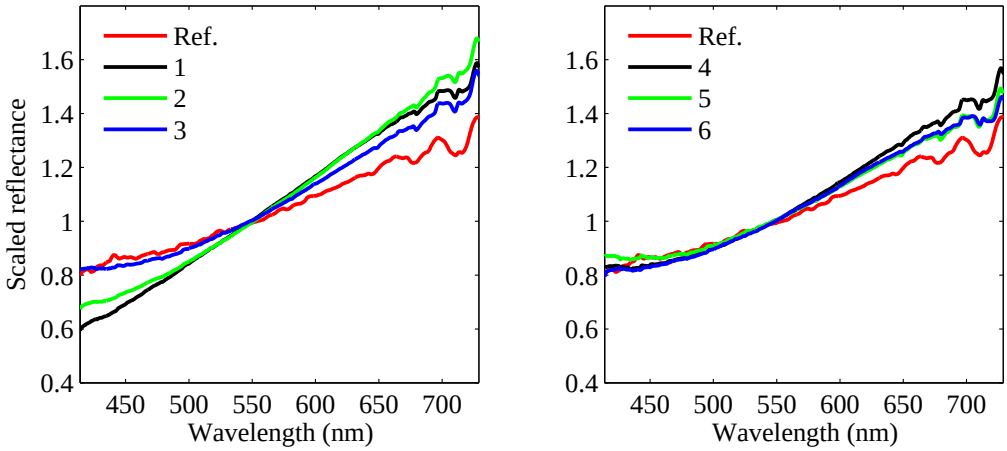


(b) Scaled reflectance spectra.

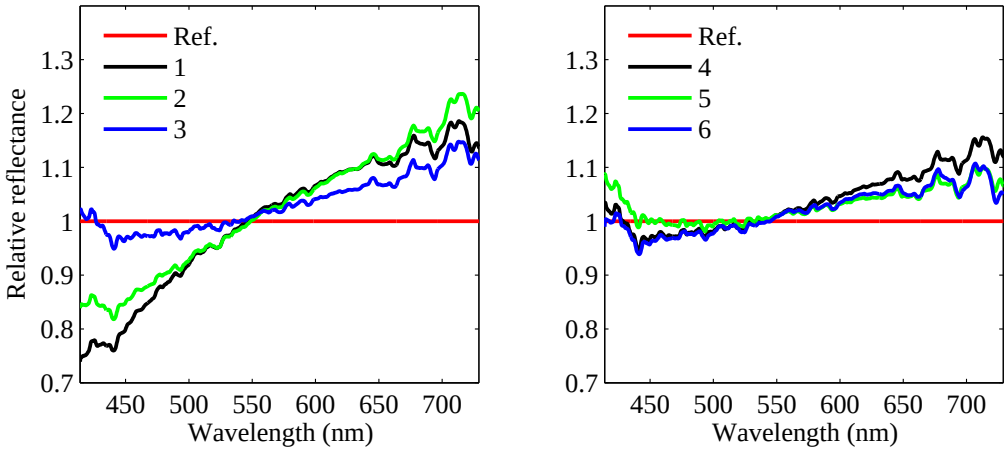


(c) Relative reflectance spectra.

**Figure 5: Measurements of the Anik F1 spacecraft collected with the DAO 1.8m telescope on 21 Aug 2014.**

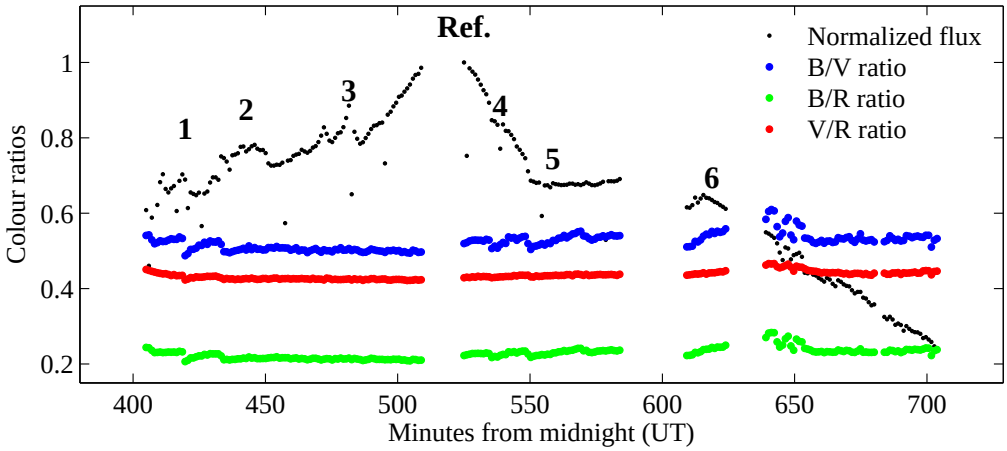


(a) Broadband lightcurve and colour ratios.

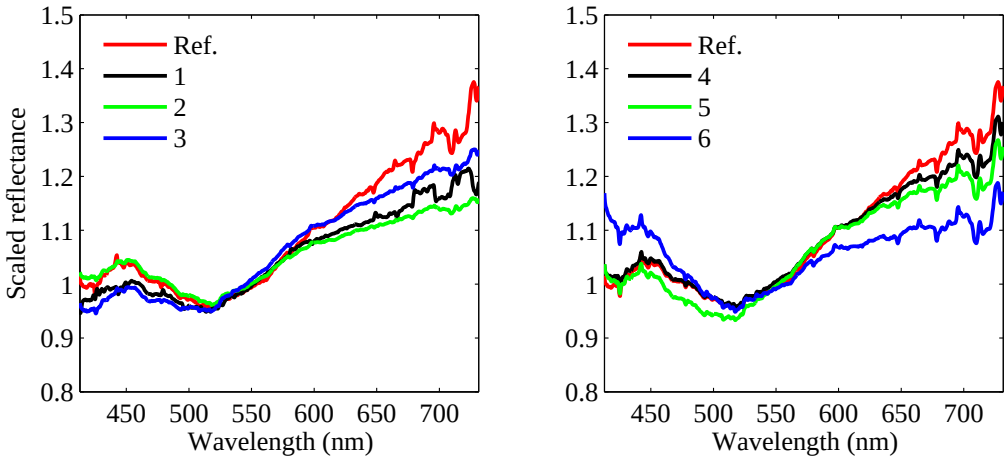


(b) Scaled reflectance spectra.

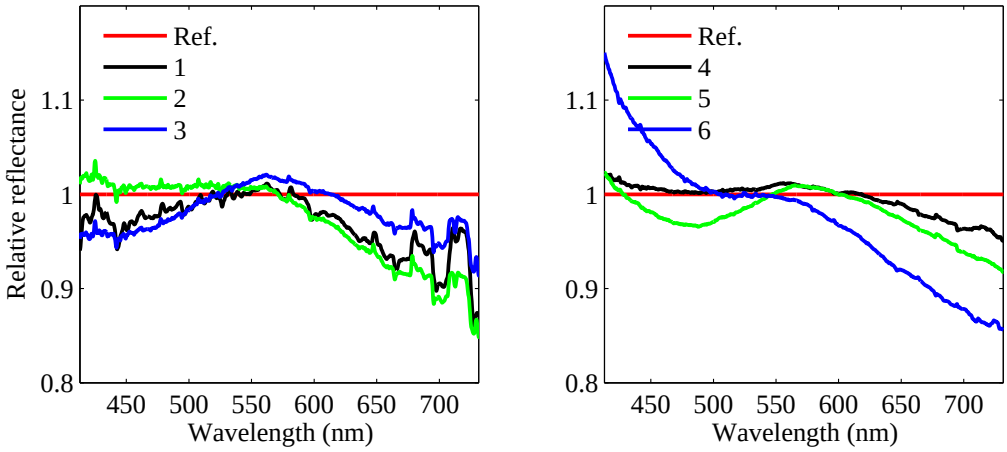


(c) Relative reflectance spectra.

**Figure 6: Measurements of the Ciel 2 spacecraft collected with the DAO 1.8m telescope on 17 Aug 2014.**

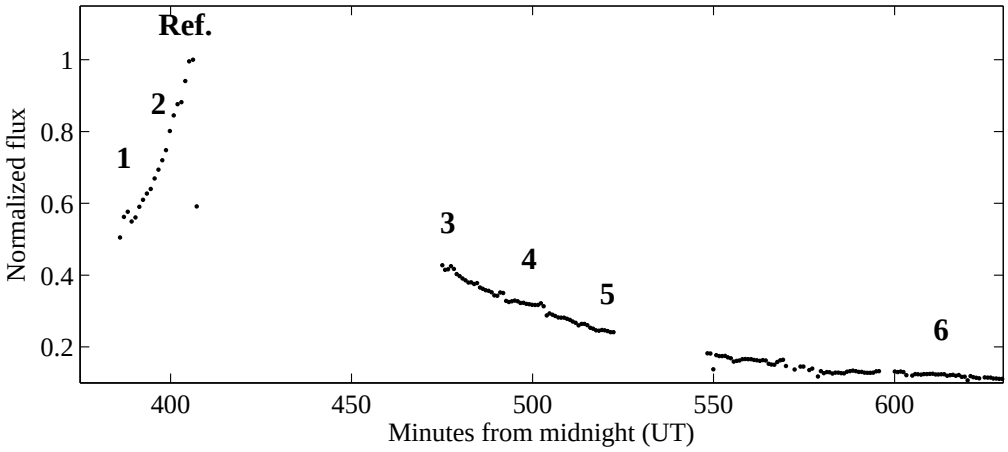


(a) Broadband lightcurve.

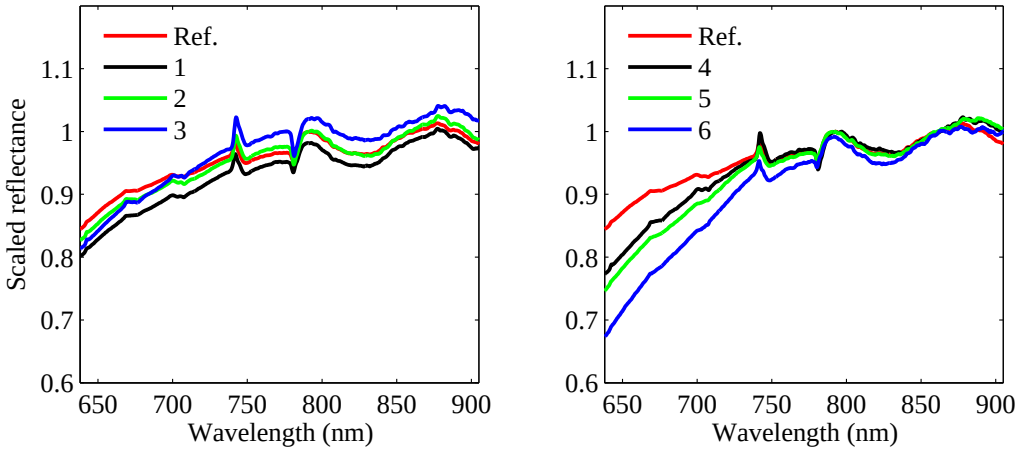


(b) Scaled reflectance spectra.

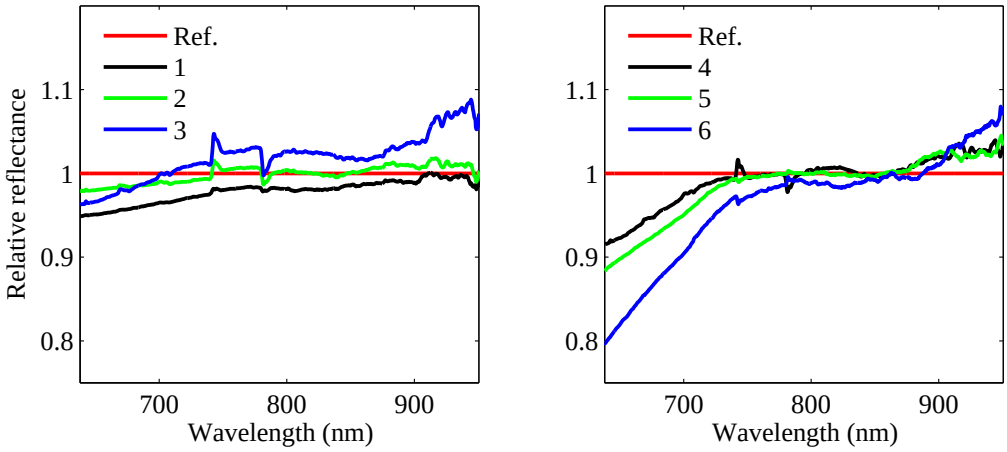


(c) Relative reflectance spectra.

**Figure 7: Measurements of the Anik G1 spacecraft collected with the DAO 1.8m telescope on 11 March 2014.**

or indicates that the material surfaces responsible for each intensity peak are not composed of the same material types or may not be represented in the same percentage. The seven different reflectance spectra shown in Fig. 8(b) provide some information as to the material composition of the two bright peaks. While measurements #1 through #4 and #6 are sloped and featureless, the Reference measurement and #5 have very flat shapes. Moreover, for both measurements, there appears to be a broad absorption feature that begins at approximately 800 nm. Based one the slope of the spectral reflectance for the Reference and #5 and on this possible absorption feature, these two measurements exhibit a similar spectral BRDF to that of the bare aluminum mirror presented in 3(a). It is noted here that the Galaxy 11 spacecraft, like the Anik F1, is based on the Boeing BSS-702 bus with the solar concentrator array. The concentrator array consists of a solar array with a reflective aluminum panel on each side [22]. Therefore the aluminum reflectance spectra obtained for the Reference measurement and #5 appears to confirm that the two intensity peaks seen in the broadband photometric lightcurve are caused by specular reflections from the aluminum panels on each side of the solar array. These results, if correct, imply that the spectral measurements centered between those peaks, such as measurement #4, should correspond to those of the solar array or a combination of the solar array and the aluminum panels. Furthermore, using the data in Figs. 1 and 3(a), the decrease in detected intensity between the two peaks of the broadband photometric lightcurve in Fig. 8(a) can be explained by the fact that an aluminum mirror is significantly more reflective than TJPV cells. At this time, the authors are at a loss to explain why similar results were not obtained for the Anik F1 spacecraft which is based on the same satellite bus. Overall, the Galaxy 11 results are encouraging and show the advantages of using the various data products that were derived from spectrometric measurements during the data interpretation stage of the experiment. Future observational experiments, as well numerical modeling ones, are needed to confirm the results presented here and to see if they can be reproduced for other satellites.

## 7 FUTURE WORK

At the present time there are three specific research areas that will be pursued. First, the elaboration of physics-based reflectance model to study and predict the spectral reflectance of artificial Earth-orbiting objects needs to be seriously considered. The results presented in Section 6 have shown that, in some cases, material type identification from reflectance spectra is possible, but this is seldom the case, even when the experiment is specifically designed to detect materials with easily recognizable spectral features. The reasons why this is the case are not understood and a reflectance model would most likely be an efficient tool to gain a better understanding of this problem.

The second area of research will be the continuation of observational experiments focused on obtaining reflectance spectra. The observational experiment discussed in the paper have yielded interesting results but it is quite clear that more spectrometric measurements of other spacecraft will be required. In addition, the results obtained from the use of colour ratios, especially those collected with the OMM telescope, indicate that the use of small aperture telescopes collecting photometric measurements of the same object simultaneously in different colour bands appears to be an interesting alternative to spectroscopy. Accordingly, future observational experiments will necessarily include research activities using the three small aperture telescopes located on the campus of Royal Military College of Canada (RMCC).

The final area of work will consist in the development of an open-access spectral library of spacecraft materials that will allow the scientific community to compare results derived from spectrometric measurements of artificial Earth-orbiting objects to the spectral BRDF of a wide variety of materials commonly found on the surfaces of spacecraft. This type of resource will be critical if the this community is expected to collaborate in trying to address the problems associated with the surface properties of space debris objects.

## 8 CONCLUSION

Results from a spectrometric characterization survey of active geostationary spacecraft has been presented here. The primary objective of the observational experiments conducted at the DAO and the OMM was to detect the presence of specific material types in the spectra of this class of satellite. While most of the reflectance spectra that have been processed so far have yielded no discernible spectral features that can be associated with specific material types, the presence of solar cells, MLI, and aluminum is believed to have been identified in the reflectance spectra of at least three satellites, namely Ciel 2, Anik G1 and Galaxy 11. Future work will seek to confirm these possible material detections through continued spectrometric observations

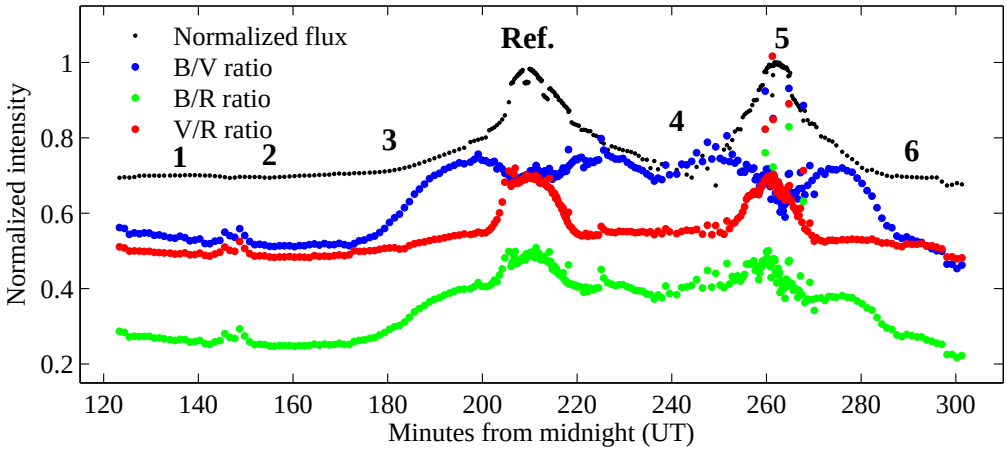


(a) Broadband lightcurve and colour ratios.

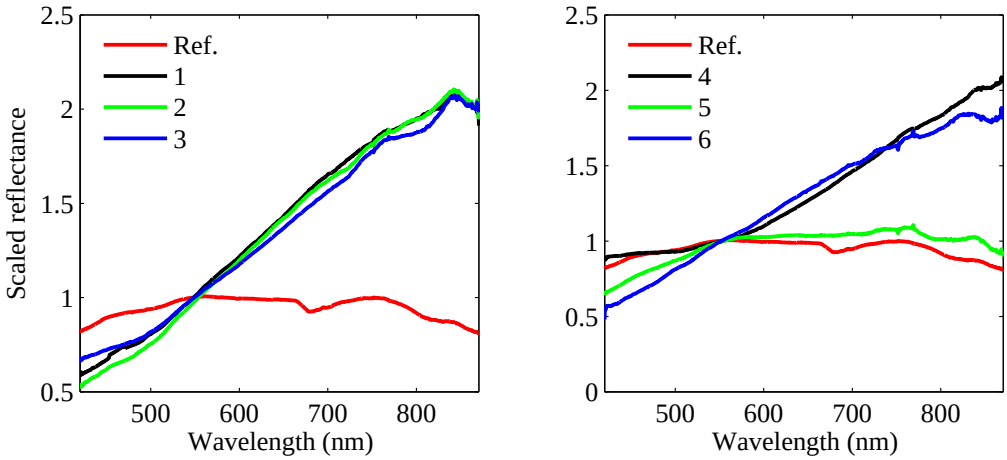


(b) Scaled reflectance spectra.

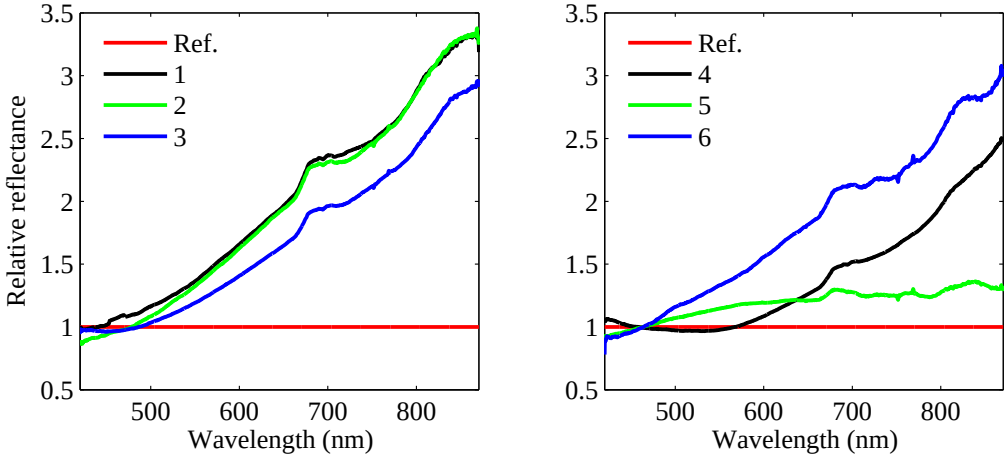


(c) Relative reflectance spectra.

**Figure 8: Measurements of the Galaxy 11 spacecraft collected with the OMM 1.6m telescope on 22 July 2014.**

of geostationary satellites and by seeking to model reflectance spectra from these types of objects. Time-resolved broadband photometric light curves and colour ratios derived from the reflectance spectra have been presented as analysis tools that can be employed to learn more about the spectral reflective properties of the studied objects and how they vary as a function of time. Another tool that was presented here and used to the same effect, namely the calculation of relative spectra, compares spectra collected at different times to one reference measurements and allows for a visual interpretation of how the SED varies between two different observations. In the end, the results presented in this paper show promise for the use of astronomical reflectance spectroscopy to identify the surface material composition of artificial Earth-orbiting objects. They also point to the fact that there is a considerable amount of research required before this technique, applied to SSA, is demonstrated to be consistent and reliable.

## 9 ACKNOWLEDGEMENT

The research presented in this paper was funded in part by the office of the Director General (Space) of the Canadian Department of National Defence and Defence Research & Development Canada.

## 10 References

[1] T. Schildknecht, R. Musci, W. Flury, J. Kuusela, J. de Leon, and L. de Fatima Dominguez Palmero. Optical Observations of Space Debris in High Altitude Orbits. In *Proceedings of the Fourth European Conference on Space Debris*, Darmstadt, Germany, 18-20 April 2005. Maui Economic Development Board, Inc.

[2] T. Schildknecht, R. Musci, W. Flury, J. Kuusela, J. de Leon, and L. de Fatima Dominguez Palmero. Properties of the high area-to-mass ratio space debris population in geo. In *Proceedings of the 2005 AMOS Technical Conference*, Kihei, Maui, HI, 2005. Maui Economic Development Board, Inc.

[3] M.J. Gaffey, E.A. Cloutis, M.S. Kelley, and K.L. Reed. Asteroids iii. chapter Mineralogy of Asteroids, pages 183–204. University of Arizona Press, 2002. URL `http://www.lpi.usra.edu/books/AsteroidsIII/pdf/3024.pdf`.

[4] J.V Lambert. Measurement of visible reflectance spectra of orbiting satellites. Master's thesis, Air Force Institute of Technology, Wright-Patterson AFB, OH, 1971. URL `http://www.dtic.mil/dtic/tr/fulltext/u2/726988.pdf`.

[5] K. Jorgensen, J. Africano, K. Hamada, P. Sydney, E. Stansbery, P. Kervin, D. Nishimoto, J. Okada, T. Thumm, and K. Jarvis. Using AMOS Telescope for Low Resolution Spectroscopy to Determine the Material Type of LEO and GEO Objects. In *Proceedings of the 2001 AMOS Technical Conference*, Kihei, Maui, HI, 2001. Maui Economic Development Board, Inc.

[6] K. Jorgensen, G. Stansbery, J. Africano, K. Hamada, P. Sydney, and P. Kervin. Most recent findings from the NASA AMOS Spectral Study (NASS): Squiggly lines lead to physical properties of orbiting objects. In *Proceedings of the 2002 AMOS Technical Conference*, Kihei, Maui, HI, 2002. Maui Economic Development Board, Inc.

[7] K. Jorgensen, J. Okada, L. Bradford, D. Hall, J. Africano, K. Hamada, P. Sydney, G. Stansbery, and P. Kervin. Obtaining material type of orbiting objects through reflectance spectroscopy measurements. In *Proceedings of the 2003 AMOS Technical Conference*, Kihei, Maui, HI, 2003. Maui Economic Development Board, Inc.

[8] K.J. Abercromby, J. Okada, M Guyote, K. Hamada, and E. Barker. Comparisons of ground truth and remote spectral measurements of the formosat and ande spacecraft. In *Proceedings of the 2006 AMOS Technical Conference*, Kihei, Maui, HI, 2006. Maui Economic Development Board, Inc. URL `http://www.amostech.com/TechnicalPapers/2006/NROC/Abercromby.pdf`.

[9] K.J. Abercromby, K. Hamada, M Guyote, J. Okada, and E. Barker. Remote and ground truth spectral measurement comparisons of formosat iii. In *Proceedings of the 2007 AMOS Technical Conference*, Kihei, Maui, HI, 2007. Maui Economic Development Board, Inc. URL `http://www.amostech.com/TechnicalPapers/2007/NROC/Abercromby.pdf`.

[10] T. Schildknecht, A. Vannanti, H. Krag, and C. Erd. Reflectance spectra of space debris in geo. In *Proceedings of the 2009 AMOS Technical Conference*, Kihei, Maui, HI, 2009. Maui Economic Development Board, Inc. URL http://www.amostech.com/TechnicalPapers/2009/Orbital_Debris/Schildknecht.pdf.

[11] P. Seitzer, S. Lederer, H. Cowardin, T. Cardona, E.S. Barker, and K.J. Abercromby. Visible light spectroscopy of geo debris. In *Proceedings of the 2012 AMOS Technical Conference*, Kihei, Maui, HI, 2012. Maui Economic Development Board, Inc. URL http://www.amostech.com/TechnicalPapers/2012/Orbital_Debris/SEITZER.pdf.

[12] D. Bédard and M. Lévesque. Analysis of the canx-1 em spectral reflectance measurements. *Journal of Spacecraft and Rockets*, 2014. doi: 10.2514/1.A32643. URL http://arc.aiaa.org/doi/abs/10.2514/1.A32643.

[13] D. Bédard. *Spectrometric Characterization of Artificial Earth-Orbiting Objects: Laboratory and Observational Experiments*. PhD thesis, Royal Military College of Canada, September 2013.

[14] E.H. Richardson. The Spectrographs of the Dominion Astrophysical Observatory. *Journal of the Royal Astronomical Society of Canada*, 62:313, 1968.

[15] J.B. Oke. Faint spectrophotometric standard stars. *The Astronomical Journal*, 99, 1990. doi: 10.1086/115444.

[16] T.L. Farhman, D.G. Schleicher, and M.F. A'Hearn. The HB Narrowband Comet Filters: Standard Stars and Calibrations. *Icarus*, 147, 2000.

[17] P. Massey. A User's Guide to CCD Reduction with IRAF. 1997.

[18] P. Massey, F. Valdes, and J. Barnes. A User's Guide to Reducing Slit Spectra with IRAF. 1992.

[19] S.J. Bus, F. Vilas, and M.A Barucci. *Asteroid III*, chapter Visible-Wavelength Spectroscopy of Asteroids, pages 169–182. The University of Arizona Press, 2002. URL http://www.lpi.usra.edu/books/AsteroidsIII/pdf/3032.pdf.

[20] M.S. Bessel. UBVRI photometry with a Ga-As photomultiplier. *Astronomical Society of the Pacific*, 88: 557 – 560, 1976. doi: 10.1086/129984. URL http://adsabs.harvard.edu/abs/1976PASP...88..557B.

[21] F.J. Vrba, M.E. DiVittorio, R.B. Hindsley, H.R. Schmitt, J.T. Armstrong, P.D. Shankland, D.J. Hutter, and J.A. Benson. A Survey of Geosynchrononous Satellite Glints. In *Proceedings of the 2009 AMOS Technical Conference*, Kihei, Maui, HI, 2011. Maui Economic Development Board, Inc. URL http://www.amostech.com/TechnicalPapers/2009/Non-resolved_Object_Characterizaion/Vrba.pdf.

[22] R. Stribling. Hughes 702 concentrator solar array. In *Photovoltaic Specialists Conference, 2000. Conference Record of the Twenty-Eighth IEEE*, pages 25–29, 2000. doi: 10.1109/PVSC.2000.915745.